Contents lists available at Science-Gate

International Journal of Advanced and Applied Sciences

Journal homepage: http://www.science-gate.com/IJAAS.html

A comparative study of titanium dioxide preparation methods in solar cells based on the TiO_2 semiconducting polymer heterojunction

H. Al-Dmour *

Department of Physics, Faculty of Science, Mu'tah University, Mu'tah, Jordan

ARTICLE INFO

Article history:
Received 29 April 2020
Received in revised form
30 July 2020
Accepted 12 August 2020

Keywords:
Solar cell
Morphology
Power conversion efficiency
Charge separation
Rectification ratio

ABSTRACT

The influence of the morphology and thickness of titanium dioxide (TiO_2) films in solar cells based on dioxide materials-semiconducting polymer was investigated. These parameters can significantly impact the mechanism of charge generation in double-layer solar cells. TiO_2 films were deposited on glass surfaces using two different techniques. Atomic force microscopy examination revealed a crystalline structure in the thick TiO_2 film produced using the doctor blade technique, whereas an amorphous structure and thin layer were obtained via the spin-coating technique. Under light conditions, the best performance between the two solar cells was obtained with the amorphous TiO_2thin film, which displayed a higher short circuit current density and power conversion efficiency (J_{sc}=1mA/cm^2, μ=0.24%) than the nanocrystallineTiO_2 solar cell (J_{sc}=0. 23mA/cm^2, μ=0.1%). This is explained by the improved efficiencies of hole-electron pair separation and charge collection through reductions in the resistance across the bulk region and in charge recombination at the interfacial layer in the amorphous solar cell. However, the high rectification ratio and high turn-on voltage under dark conditions, and forward bias current in the nanocrystalline solar cell led to an increase of 0.3 V in the open circuit voltage in comparison with the amorphous device. These results confirm that, for double-layer solar cells, an amorphous thin film performs better than a thick nanocrystalline TiO_2 layer, in contrast to previous observations for dye-sensitized solar cells.

1. Introduction

In the last two decades, solar cells based on the TiO_2 semiconducting polymer heterojunction have attracted significant attention because of their high power conversion efficiencies compared with other types of solar cells (Thu et al., 2018). Several techniques have been applied to improve the performance of polymer-metal oxide solar cells, exploiting the characteristics of their components. Metal oxides semiconductors (MOSs) have been widely studied as the electron transport layer, including CeO_2, TiO_2, ZnO, and SnO_2 (Vittal and Ho, 2017). Their high electron mobilities, good pore filling, and wideband gaps make MOSs very attractive for electronic and optoelectronic applications such as solar cells and sensors. They can be used as a layer deposited directly onto a transparent conductive oxide (TCO) substrate or mixed with a hole conductor to increase the solar cell's efficiency (Shirkavand et al., 2019). Additionally, these materials have a sufficient offset of the lowest occupied molecular orbital (LUMO) of the hole transport material (HTM) to provide enough energy to separate the electron-hole pair at the interfacial layer (Cheema and Joya, 2018). O'Regan and Grätzel (1991) fabricated a high-efficiency solar cell using a nanocrystalline nc-TiO_2 electron transport layer because of its high chemical and optical stability, nontoxicity, low cost, and corrosion resistance in comparison to other types of MOs. Additionally, good light harvesting and increased photoinduced charge separation were accomplished by optimizing the morphology and thickness of the nc-TiO_2.

These physical attributes play important roles in improving the efficiency of dye-sensitized solar cells (DSSCs) by increasing the absorption of dye at the surface of the TiO_2 and interfacial layer using nc-TiO_2. In the absence of a dye, however, that will be a disadvantage in making solar cells because there is increased aggregation at the interface between the hole transport layer and TiO_2.In this article, we

* Corresponding Author.
Email Address: hmoud79@mutah.edu.jo
https://doi.org/10.21833/ijaas.2020.12.015
Corresponding author's ORCID profile:
https://orcid.org/0000-0001-5680-5703

report our study of the fabrication, characteristics, and structural properties of TiO_2layers produced using two different deposition methods for solar cell application. We confirm that amorphous TiO_2/polymer solar cells show better performance in comparison to nc-TiO_2 solar cells.

2. Experimental method

2.1. Sintering of titanium dioxide films

Two devices were fabricated using an active layer sandwiched between the bottom and top electrodes. The first device had a thin layer of TiO_2 coated on a pre-cleaned fluorine-doped conducting tin oxide (FTO) glass plate (sheet glass, 8 Ω/sq, Solaronix com). The TiO_2solution (5mL, Solaronix com) was dropped onto the bottom electrode and, within a few seconds, was spun at 1000 rpm for 60 s. For the second device, a thick layer of nc-$TiO_2$was produced by depositing TiO_2 sol gel (50µL, Solaronix com) on the edge of the bottom substrate using a micropipette; then, a cleaned glass rod was used to spread the sol gel over the electrode substrate area defined by tape (Shirkavand et al., 2019). This film was left to dry in air for 10 min until its milky color disappeared. The tape was then removed, and the substrate placed on a hot plate preheated between 75^0Cand 100^0C (limited by the accuracy of the dial setting) for 30 min. For both devices, the left on the hot plate for 110 min, during which time the temperature was increased from ~75^0C to 450^0C in 4 steps. Finally, heating was stopped and the temperature allowed to fall naturally to ~70^0C, where upon the substrate was recovered.

2.2. Preparation of poly (3-hexylthiophene) (P3HT) Film

Poly (3-hexylthiophene) was chosen as the organic semiconductor for the second part of device components because it h has been widely used in polymer-based electronics such as transistors and solar cells (Yang et al., 2017). The P3HT solution for spin coating was prepared by weighing regioregular poly (3-hexylthiophene-2,5-diyl) (0.1g, Sigma-Aldrich) into a 5 mL volumetric flask, and then topping up with chloroform (Aldrich Chemical, UK). To enhance the solubility of P3HT in chloroform, the volumetric flask was placed in a warm ultrasonic bath at ~50°C and sonicated for 30–60 min. Undissolved particles were removed by passing the solution via a syringe through a 0.2µm PTFE filter into a clean vial. To prepare the P3HT layers in the two devices, each substrate was placed on the vacuum chuck of a photo resist spinner (Model 4000, Electronic Micro Systems Ltd.). A pre-cleaned glass pipette was used to drop the P3HT solution (5mL) onto either the nc-TiO_2or thin TiO_2 layer. After several seconds, the substrate was spun at 1000 rpm for the 60s.

2.3. Device characterization

The substrates were removed and stored in the dark until gold electrodes were deposited onto the P3HT layers. The current-voltage characteristics of the solar cells were evaluated using a Keithley model 4200 source-measure unit, which was capable of applying negative and positive voltages in the range of +1 to −1V to the device and measuring currents in the range of 1pA to 1mA. The optical responses of the solar cells were obtained using a tungsten lamp. The light was focused onto the transparent FTO electrode with an incident power of 72mW/cm^2, constrained by an aperture to fall on an area coinciding with one of the gold top electrodes.

3. Results and discussion

Fig. 1 shows the semilog plots of current density (J) versus voltage (V) applied for the P3HT/amorphousTiO_2 solar cell when the voltage was swept from−1 to 1 V under different conditions. In the dark, the current is higher when the bias was swept from 0 to 1 V compared to the opposite sweep direction. The rectification ratio is defined as the forward current I_F divided by the reverse current I_S at a ±1 V bias. As can be seen from Fig. 1, the J-V characteristics of the P3HT/amorphous TiO_2 solar cell display rectification with a turn-on voltage for the solar cell of~0.75V. Additionally, the rectification ratio is estimated to be ~10^2 at ±1V. Under illumination, the rectification ratio nearly disappears, and the current increases from 7×10^6 to 1mA/cm^2 at −1V. This is attributed to the change in conductivity of the bulk region at the interface inside the solar cell. For the region between −1 to 0 V (under the reverse bias condition), the photo conductivity mode governs the increase of the photocurrent. This depends on the generation of free charges through the absorption of the incident of photos and their transport under the influence of the electric field and bulk-region capacitance. In contrast, there was a small increase in forward bias current under illumination, from the turn voltage to +1V related to the small enhancement of majority charge carriers, which was already high in the dark.

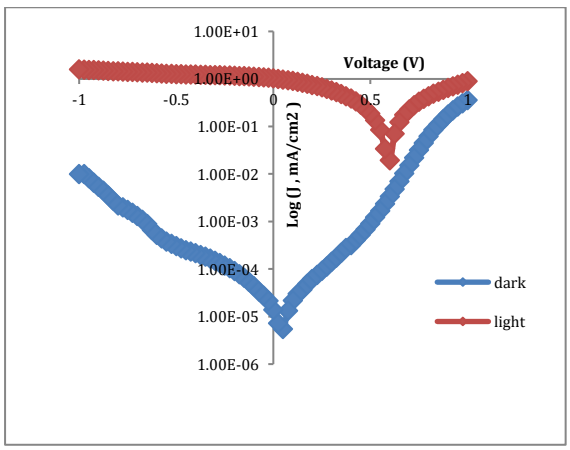

Fig. 1: Log current density–voltage characteristics of the P3HT/amorphous TiO_2 solar cell

Fig. 2 shows the *J-V* characteristics of the P3HT/amorphous TiO_2 solar cell in the forward applied bias region of 0 to 1V on a linear scale. From Fig. 2, the J_{SC} and open-circuit voltage (V_{OC}) are 1mA/cm^2 and 0.6 V, respectively. The power conversion efficiency (μ) and fill factor (*FF*) of the amorphous solar cells were calculated using Eq. 1 and 2,

$$\mu = \frac{J_{max}V_{max}}{P_L} \quad (1)$$

$$FF = \frac{J_{max}V_{max}}{J_{sc}V_{oc}} \quad (2)$$

where P_L is light intensity falling on the device, and J_{max} and V_{max} are the current and voltage corresponding. Using the data obtained from Fig. 2 (J_{max}=0.571mA/cm^2 and V_{max}=0.3V), the values of μ, and *FF* were determined as 0.24% and 28 %, respectively.

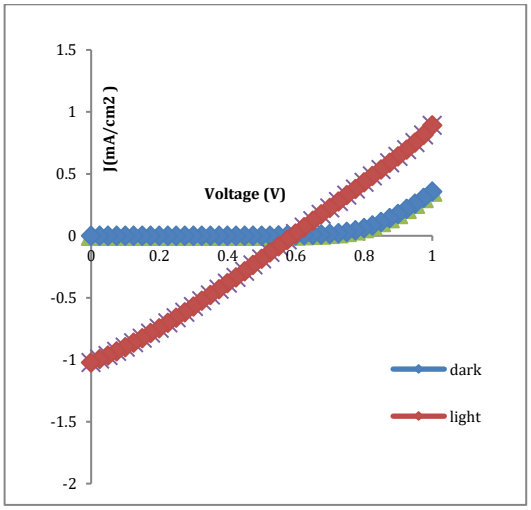

Fig. 2: Current density–voltage characteristics of the P3HT/amorphous TiO_2 solar cell

The performance of the P3HT/nanocrystalline TiO_2solar cell was next investigated. Fig. 3 shows the semilog plots of *J* versus *V* for this device under dark and light conditions when the voltage was swept from 1 to −1V. The reverse bias current (from 0 to −1V) is lower compared to the opposite sweep direction; however, in the negative region, the current is nearly constant with increasing applied voltage. In contrast, the forward current of the nc-TiO_2 solar cell increases with the applied voltage and is lower than that in the amorphous solar cell. Thus, a higher rectification of ~10^3 at ±1 V is observed in the nc-TiO_2 solar cells, arising from the difference in the energy bands of the materials used to fabricate the cell. These results agree with those of Hwang and Lee (2008), who observed a similar high rectification ratio due to the best crystallization in p–n junction diode. Additionally, the turn-on voltage of the nc-TiO_2 solar cell is 0.635V higher than the amorphous solar cells. On the other hand, when the device was under illumination, the reverse current significantly increases in revere current more than four orders of magnitude, whereas the current in the forward direction is almost unchanged for the region between 0.85 and 1 V, under the effect of photoconductivity.

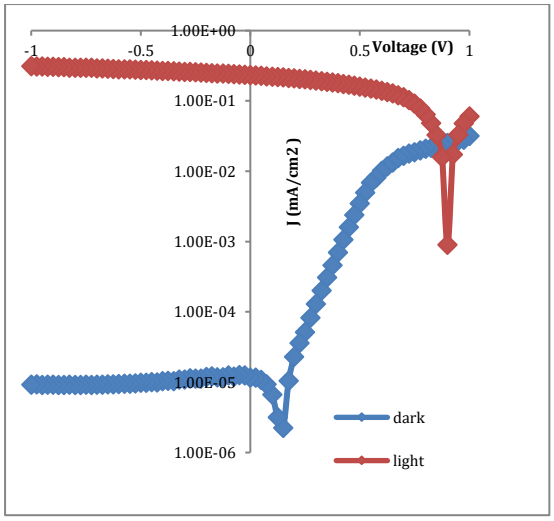

Fig. 3: Log current density–voltage characteristics of the P3HT/nc-TiO_2 solar cell

To compare the efficiencies of amorphous solar cells, the *J-V* characteristics of the P3HT/nc-TiO_2solar cell were also studied under dark and light conditions (Fig. 4) in the forward bias region of 0 to 1V. This solar cell exhibits a J_{SC} value of 0.23mA/cm^2, which is substantially lower than that of the amorphous TiO_2 solar cell (1mA/cm^2). Thus, the nc-TiO_2-based device produces a low μ of 0.1%, even though its V_{OC} and *FF* values are 0.8 V and 40%, respectively.

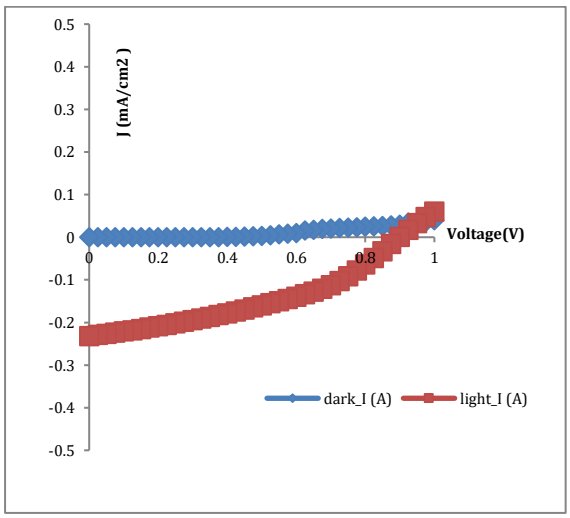

Fig. 4: Current density–voltage characteristics of the P3HT/nc-TiO_2 solar cell

Under dark conditions, the *J-V* characteristics of the amorphous and nanocrystalline TiO_2 solar cells exhibit exponential behavior at low voltage and non-linear behavior at high voltage. Thus, at low voltage, both cells exhibit typical diode-like behavior in the dark, such that the forward current is solely controlled by thermionic emission theory (Bartolomeo, 2016). According to this theory, the relationship between the voltage and dark current density is given by Eq. 3 and 4:

$$J = J_O \exp\left(\frac{-qV_B}{nkT}\right) \quad (3)$$

with

$$J_0 = A * T^2 \exp\left(\frac{-q\phi_B}{kT}\right) \quad (4)$$

where n is the ideality factor, k is the Boltzmann constant, q is the electronic charge, A^* is the Richardson constant, T is the temperature, and Vb is the potential barrier height. From Eq. 3, the ideality factor can be determined from the slope of the exponential regime of the semi-logarithmic plot of the dark J–V characteristics, and can be expressed as:

$$n = \frac{q}{KT}\frac{dv}{d(\ln J)} \quad (5)$$

If n is equal to unity (n=1), the device behaves as an ideal diode in which there is no trapping or recombination of charge carriers, nor the presence of high series resistance or interfacial layers. For example, Kim observed that the ideality factor of an Au/Al_2O_3 device was ~ n=2 for an Al_2O_3 thickness up to 4.9nm, but increased to n=2.9 at an Al_2O_3 thickness of 8.3 nm (Kim et al., 2018). Using equation 5, we calculated the ideality factors for the prepared amorphous and nc-TiO_2 solar cell devices, obtain in values of 1.58 and 3, respectively. These results may be attributed to drop bias voltage cross the series resistance of the bulk region in the device and interfacial layer or depletion region between the P3HT and nc-TiO_2. In addition, the thickness of the bulk region and the large interfacial layer of the junction in the nc-TiO_2 solar cell increases the ideality factor compared to the other device. This indicates to increase in the electron/hole recombination dominated at a high interfacial layer between P3HT and nc-TiO_2 layers. However, our previous report showed that a potential interfacial barrier might be formed between the P3HT and nc-TiO_2, which was interpreted as the origin of the observed rectification (Al-Dmour and Taylor, 2009). Rectification depends on the energy level alignment between the P3HT and nc-TiO_2. And/or the work functions of the bottom and top electrodes. When V>0 is applied to the device, the Au electrode is forward-biased, and the current characteristics are dominated only by the series resistance of the bulk region, with decreased shunt resistance at the interface. Thus, the results here imply that a thicker layer of TiO_2 reduces the dark current and gives rise to high rectification.

Fig. 5 shows the tapping–mode atomic force microscopy (AFM) images of the two TiO_2 films. There is a significant difference in their topographies, such as their surface roughness, grain formation, and thickness. In the amorphous TiO_2 film, the surface is nearly flat with low roughness and a thickness of less than 100nm. In contrast, greater differences are seen in the nc-TiO_2 film, which has a root-mean-square (RMS) roughness of 20.5 nm, a mean particle height of 86 nm, and a thickness of 2μm. These findings confirm that, for the nc-TiO_2, inclusions of anatase TiO_2 phases appear when the film thickness is larger, in comparison with the amorphous TiO_2 film.

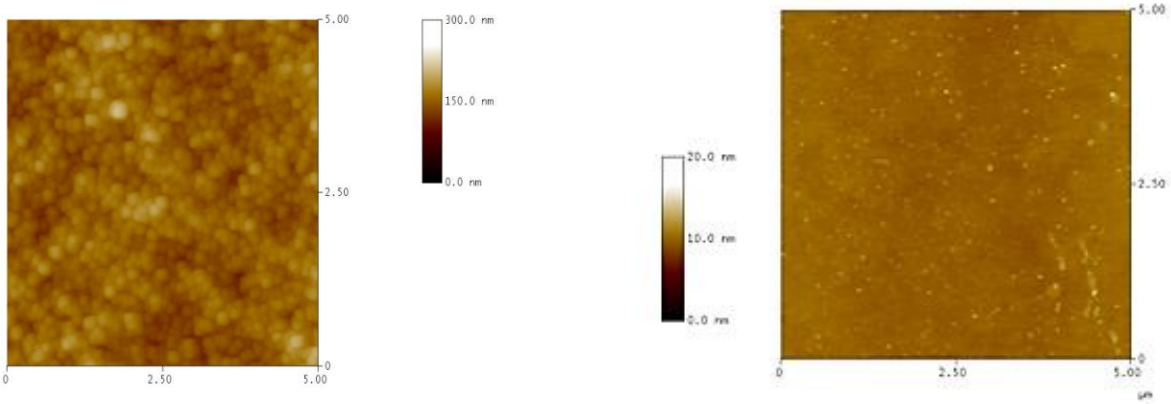

a: AFM image of nanocrystalline TiO_2 film

b: AFM image of amorphousTiO_2 film

Fig. 5: AFM image

Several studies have examined the surface properties and thicknesses of TiO_2 films to improve the power conversion efficiencies of metal-oxide-based solar cells (Liu et al., 2018). Here, we find that the thinner layer and flatter, smoother surface of the amorphous TiO_2 are much better for producing a photocurrent than the nanocrystalline TiO_2 having a rough surface and large interfacial layer at the junction in solar cells. The power conversion efficiency of a solar cell depends on the efficiencies of five processes, which are described in Eq. 6 as:

$$\mu = (1 - R)\mu_{\mathrm{AB}}\mu_{\mathrm{ED}}\,\mu_{\mathrm{CT}}\mu_{CC} \quad (6)$$

where μ_{AB} is the efficiency of light absorption in the active layer; μ_{ED} is the efficiency of exciton migration to the interface; μ_{CT} is the efficiency of charge dissociation at the interface and transport to the electrodes; μ_{CC} is the efficiency of charge collection; and R is the reflectivity of the substrate at the air interface. The highest efficiencies among these five processes are charge dissociation and charge collection for the thin amorphous solar cell, whereas the efficiency of light absorption is highest for the

thick nc-TiO_2 solar cell. For the amorphous TiO_2 solar cell, there is enough separation energy stemming from the work function difference of the two electrodes and semiconductor in addition to the interfacial layer at the junction to separate the electron-hole pairs. Thus, they require less time to flow electron and holes out of the device as current. In contrast, in the nanocrystalline solar cell, the contribution of the work function difference between the electrodes in charge separation is limited, and coupled with the increase in the series resistance of the bulk region, increased charge carrier recombination is observed. Thus, we have observed the power conversion efficiency of the amorphous solar cell is enhanced.

Fig. 6 shows the power characteristics of the two devices as a function of voltage. The results confirm that the amorphous TiO_2 solar cell produces a high maximum electric power of 0.18mW/cm^2 as compared to 0.06mW/cm^2 for the nanocrystalline solar cell. On the other hand, the range of operation of solar cells starts from zero voltage to open circuit voltage, which was small in amorphous TiO_2 solar cells. That confirms the difference in interfacial layers, which affect the hole–electron separation.

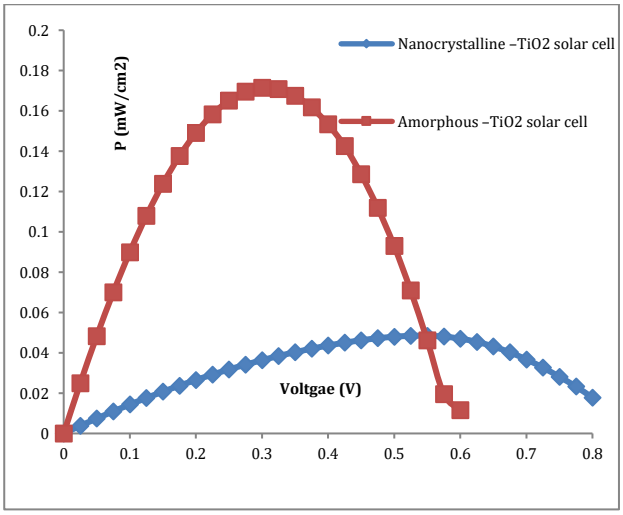

Fig. 6: Power versus voltage characteristics of nanocrystalline and amorphous TiO_2 solar cells

The observed results confirm the importance of the thickness and morphology of the TiO_2 on the performance of a solar cell in agreement with the results reported by other research groups. For example, Boroomandnia et al. (2015) studied different types of TiO_2 films and their effects on the performance of solar cells. It was found higher densities of TiO_2 solar cells produce lower power conversion efficiency than TiO_2 nano particles solar cells (Boroomandnia et al., 2015). That is attributed to the difference in the interface area in tow devices. Finally, Al-Attafi et al. (2018) used a similar approach to our work to study the effect of amorphous TiO_2 on DSSC performance. A detrimental effect on DSSC performance was investigated with the amorphous material in contrast to the observations here in for double layer solar cells (Al-Attafi et al., 2018).

4. Conclusion

Amorphous TiO_2 solar cells offered better performance than nanocrystalline TiO_2 solar cells under light conditions. The amorphous TiO_2 solar cells generated a high power conversion efficiency (of 0.24% and a short current density *J*sc of 1mA/cm^2, which were due to the improved efficiencies of hole-electron pair separation and charge collection through the reductions of resistance across the bulk region and charge recombination at the interfacial layer. The dark current results emphasized the effect of the TiO_2 structure in terms of the high rectification ratio and low reversed bias current observed in the nanocrystalline solar cell.

Compliance with ethical standards

Conflict of interest

The authors declare that they have no conflict of interest.

References

Al-Attafi K, Nattestad A, Wu Q, Ide Y, Yamauchi Y, Dou SX, and Kim JH (2018). The effect of amorphous TiO_2 in P25 on dye-sensitized solar cell performance. Chemical Communications, 54(4): 381-384. https://doi.org/10.1039/C7CC07559F **PMid:29242873**

Al-Dmour H and Taylor DM (2009). Revisiting the origin of open circuit voltage in nanocrystalline-TiO_2/polymer heterojunction solar cells. Applied Physics Letters, 94(22): 148. https://doi.org/10.1063/1.3153122

Bartolomeo AD (2016). Graphene Schottky diodes: An experimental review of the rectifying graphene/semiconductor heterojunction. Physics Reports, 606: 1-58. https://doi.org/10.1016/j.physrep.2015.10.003

Boroomandnia A, Kasaeian AB, Nikfarjam A, Akbarzadeh A, and Mohammadpour R (2015). Effect of crystallinity and morphology of TiO_2 nano-structures on TiO_2: P3HT hybrid photovoltaic solar cells. Applied Solar Energy, 51(1): 34-40. https://doi.org/10.3103/S0003701X15010065

Cheema H and Joya KS (2018). Titanium dioxide modifications for energy conversion: Learnings from dye-sensitized solar cells. In: Yang D (Ed.), Titanium dioxide: Material for a sustainable environment: 387-420. BoD–Books on Demand, Norderstedt, Germany. https://doi.org/10.5772/intechopen.74565

Hwang JD and Lee KS (2008). A high rectification ratio nanocrystalline p–n junction diode prepared by metal-induced lateral crystallization for solar cell applications. Journal of the Electrochemical Society, 155(4): 259-262. https://doi.org/10.1149/1.2840618

Kim H, Kim Y, and Choi BJ (2018). Interfacial characteristics of Au/Al2O3/InP metal-insulator-semiconductor diodes. AIP Advances, 8(9): 095022. https://doi.org/10.1063/1.5047538

Liu H, Bala H, Zhang B, Zong B, Huang L, Fu W, and Zhan Z (2018). Thickness-dependent photovoltaic performance of TiO_2 blocking layer for perovskite solar cells. Journal of Alloys and Compounds, 736: 87-92. https://doi.org/10.1016/j.jallcom.2017.11.081

O'regan B and Grätzel M (1991). A low-cost, high-efficiency solar cell based on 19dye-sensitized colloidal TiO_2 films. Nature, 353(6346): 737-740. https://doi.org/10.1038/353737a0

Shirkavand M, Bavir M, Fattah A, Alaei HR, and Tayarani Najaran MH (2019). Influence of TiO_2 layer thickness as photoanode in dye sensitized solar cells. AUT Journal of Electrical Engineering, 51(1): 101-110.

Thu C, Ehrenreich P, Wong KK, Zimmermann E, Dorman J, Wang W, and Vasilopoulou M (2018). Role of the metal-oxide work function on photocurrent generation in hybrid solar cells. Scientific Reports, 8(1): 1-8. https://doi.org/10.1038/s41598-018-21721-2 **PMid:29476065 PMCid:PMC5824951**

Vittal R and Ho KC (2017). Zinc oxide based dye-sensitized solar cells: A review. Renewable and Sustainable Energy Reviews, 70: 920-935. https://doi.org/10.1016/j.rser.2016.11.273

Yang BZ, Lin YS, and Wu JM (2017). Flexible contact-electrification field-effect transistor made from the P3HT: PCBM conductive polymer thin film. Applied Materials Today, 9: 96-103. https://doi.org/10.1016/j.apmt.2017.06.001